UC San Diego
UC San Diego Previously Published Works

Title

Crohns Disease-associated variant in laccase domain containing 1 (LACC1) modulates T cell gene expression, metabolism and T cell function.

Permalink

https://escholarship.org/uc/item/7gh805vb

Journal

Nature Communications, 16(1)

Authors

Li, Yingcong

Ascui, Gabriel

Dicker, Martina

et al.

Publication Date

2025-03-15

DOI

10.1038/s41467-025-57744-3

Peer reviewed

Article

Crohn's Disease-associated variant in laccase domain containing 1 (*LACC1*) modulates T cell gene expression, metabolism and T cell function

Check for updates

Yingcong Li [1,2], Gabriel Ascui [1,3], Martina Dicker[1], Thomas Riffelmacher [1], Vivek Chandra [1], Benjamin Schmiedel [1], Ting-Fang Chou[1], Pandurangan Vijayanand [1,3,4,5] ✉ & Mitchell Kronenberg [1,2,5] ✉

Genome wide association studies (GWAS) identify many risks for Crohn's disease (CD), including a site near the metabolism gene laccase domain containing 1 (*LACC1*). We previously found this site near *LACC1* was associated with decreased *LACC1* expression in T lymphocytes, yet the mechanism affecting gene expression and its links to T cell function and inflammatory disease were unknown. Here we identify variants in the promoter region that influence transcription of *LACC1*. Direct association of disease-risk variants with lower *LACC1* pre-mRNA in human CD4+ T cells is confirmed by comparing transcripts from each allele from donors heterozygous for the *LACC1* CD-risk allele. Using gene editing, we validate the function of this promoter region in *LACC1* expression in T cells. Human CD4+ T cells with *LACC1* gene knockdown show altered metabolism, including reduced oxygen consumption rate, and reduced in vitro regulatory T cell differentiation. Therefore, our study provides a mechanism linking these specific *LACC1* variants to colitis by attributing promoter region variants to changes in T cell metabolism and function.

Genome wide association studies (GWAS) have implicated variants at more than 200 genetic loci as providing risks for inflammatory bowel disease (IBD)[1–4]. In most cases, however, the particular cell type(s) affected, the exact gene implicated, and the mechanism(s) of action of the variants, are unknown. In order to elucidate how a GWAS hit is related to IBD pathogenesis, we focused on the *laccase domain containing 1 (LACC1)* gene, also known as *C13ORF31* or *fatty acid metabolism – immunity nexis* or *FAMIN*[5]. Several studies have implicated a region containing this gene in the causation of Crohn's disease (CD)[1,2,6,7] and ulcerative colitis (UC)[8], with an OR in the 1.1-1.2 range.

Some of these studies[1,2,7] included rs3764147 as a CD risk; this is a coding mutation in *LACC1* substituting valine for isoleucine at position 254, which generates a hypomorphic allele. Notably, although previous studies have shown that this protein coding variant does not directly alter *LACC1* mRNA or protein expression[5,9], it causes a partial loss of immunometabolic function of the protein, which could contribute to colitis risk. Moreover, a rare, putatively disabling mutation in *LACC1*, C284R, led to early onset Crohn's disease[10]. Therefore, unlike cases in which the gene(s) affected by a single nucleotide polymorphism (SNP) in a noncoding region remains to be identified, based on the very rare

[1]La Jolla Institute for Immunology, La Jolla, CA, USA. [2]Department of Molecular Biology, University of California San Diego, La Jolla, CA, USA. [3]Department of Medicine, University of California San Diego, La Jolla, CA, USA. [4]Department of Molecular and Clinical Cancer Medicine and NIHR and CRUK Liverpool Experimental Cancer Medicine Center, University of Liverpool, Liverpool, UK. [5]These authors jointly supervised this work: Pandurangan Vijayanand, Mitchell Kronenberg. ✉e-mail: vijay@lji.org; mitch@lji.org

loss of function mutation at position 284 and hypermorphic allele at position 254, we could be reasonably confident that *LACC1* is linked to IBD. In other patients, mutations in *LACC1*, including premature stop codons, lead to juvenile idiopathic arthritis[11–14]. *LACC1* also has been linked to leprosy[15] and Behçet's disease[16] by GWAS. The outcomes illustrate the importance of *LACC1* in preventing several inflammatory diseases, and furthermore, that the type of disease that develops in response to a mutation in a particular gene are influenced by differences in other genetic loci.

LACC1 is highly expressed in myeloid cells[17], and most of the studies of its function have been in macrophages. *LACC1* has been reported to be a metabolic regulator in macrophages[5,9,18,19], but its subcellular localization[18,20] and function in metabolism are controversial. *Lacc1* deficient mouse macrophages are reported to show reduced fatty acid oxidation and altered mitochondrial morphology[5]. Subsequent evidence indicates this gene encodes an enzyme important for purine metabolism, including adenosine deaminase, purine nucleoside phosphorylase, and *S*-methyl-5'-thioadenosine phosphorylase[18]. Other reports indicate important roles for LACC1 in endoplasmic reticulum (ER) stress[21] or in the regulation of autophagy[9]. Recently, a function for LACC1 in polyamine metabolism is described[19]. Similar to the results from metabolic studies, divergent results are obtained from investigation of the influence of LACC1 on immune responses. In several cases, inflammatory responses, such as those associated with colitis, are reduced in *Lacc1*−/− mice, or in cells with reduced *LACC1* expression[22]. For example, decreased TNF, IFNγ and IL-17 are found after T cell transfer into *Rag2*−/−*Lacc1*−/− mice, and reduced IL-1β, TNF, IL-6 responses to intraperitoneal LPS injection in the absence of LACC1[22]. It is uncertain how this hypo-responsiveness leads to increased colitis, but this may be analogous to the compensatory immune response as a result of loss of function mutations in nucleotide-binding oligomerization domain-containing protein 2 (NOD2), an intracellular sensor of bacteria and other danger signals[23]. In fact, a connection between NOD2 with LACC1 to induce ER stress is observed[21]. Innate immune hypo-responsiveness is not observed in another study[9], however, and in yet another, *Lacc1*−/− bone marrow derived macrophages cultured with LPS produce increased TNF and IL-6[19]. Furthermore, serum IL-1β, IL-6, TNF, and IFN-γ levels were higher in the *Lacc1*−/− mice after dextran sodium sulfate (DSS) colitis[24], likely due in part to myeloid cell activation. Therefore, although the metabolic effects and functional findings on immunity differ greatly between studies, overall there is evidence that LACC1 regulates metabolism in ways that affect myeloid cells, such as macrophages.

The Database of Immune Cell eQTLs, Expression and Epigenomics (DICE) tests for cell type-specific expression quantitative trait loci (eQTLs) and chromatin interactions by comparing gene expression in highly purified mononuclear cell types from human peripheral blood (PBMC)[17]. The apparently healthy cohort is genotyped, permitting a comprehensive analysis that correlates, in populations, gene expression with genetic polymorphisms. Our previous analysis[3] highlights a common polymorphism, rs9567293, located approximately 6 kb upstream from the promoter of the *LACC1* gene, in a haploblock that is a significant GWAS hit region for Crohn's disease (CD) and other inflammatory conditions[17]. Unexpectedly, we observed that rs9567293 is a T and B cell specific expression quantitative trait locus (eQTL) for the *LACC1* gene. Gene expression in NK cells and classical and non-classical monocytes is not affected by this allelic variation. The disease associated rs9567293-C allele correlates with lower gene expression. Therefore, the data suggest that this common allelic variation associated with CD acts in lymphocytes. This prompted us to rigorously confirm this by measuring gene expression in heterozygous cells, to explore the molecular basis for reduced *LACC1* gene expression in rs9567293^C/C T cells, and to analyze the effects of reduced LACC1 on CD4+ T cell metabolism and function that might be linked to IBD.

Results

Reduced T cell *LACC1* expression from a disease risk allele

The CD-risk allele in the *LACC1* locus is in a complex haploblock with variants with different frequencies in strong linkage disequilibrium (LD). The well-studied CD-risk coding variant rs3764147-G, which generates a hypomorphic allele[1,2,7], is in LD (D' = 0.98, r^2 = 0.36; European population, Supplementary Fig. 1a) with the non-coding CD-risk variant rs9567293-C, which we had previously reported as a strong eQTL for *LACC1* in T cells (Supplementary Fig. 1b). However, the population frequency of the CD-risk coding variant (rs3764147-G allele) is less than that of the non-coding CD-risk variant (rs9567293-C allele), which is highlighted by the lower correlation or r^2 value between these variants, indicating that their alleles are distributed on different haplotypes within this haploblock. This results in two types of potential CD-risk alleles in the population, an allele that carries both the coding and non-coding variant (rs3764147-G allele and rs9567293-C allele) and a common CD-risk allele that carries the non-coding variant rs9567293-C allele without the coding variant (rs3764147-G allele). The opposite configuration, a coding variant creating a hypomorph without the non-coding CD-risk rs9567293-C allele, is very infrequent. Notably, even in donors without the protein-coding variant (rs3764147-A allele), the CD-risk non-coding variant (rs9567293-C allele) was associated with reduced expression of *LACC1* in T cells but not in monocytes (Supplementary Fig. 1c). Previous work shows that the protein-coding variant does not directly influence *LACC1* expression levels[5][9], while our data show the non-coding variant is an independent factor that could contribute to CD risk.

To validate if the CD-risk allele rs9567293-C reduced *LACC1* transcription in T cells specifically by influencing T cell-specific *cis*-regulatory elements or chromatin interactions, we first analyzed H3K27ac ChIP-seq for active enhancers and H3K27ac HiChIP-seq for chromatin interactions. We tested four cell types from human PBMCs: naïve CD4+ T cells, naïve CD8+ T cells, classical monocytes and NK cells. The description of the cell types and primary data were obtained from a previous publication[25]. There was a region of H3K27 acetylation near the *LACC1* promoter in all four tested cell types, including naïve CD4+ T cells (Fig. 1a) and naïve CD8+ T cells, classical monocytes and NK cells (Supplementary Fig. 1d). There also were H3K27ac HiChIP-seq peaks in classical monocytes, indicative of possible chromatin interactions. However, we did not detect significant H3K27ac peaks near rs9567293 in lymphoid cells, indicating this site was not likely to be a functional eQTL in these cell types. Given that single nucleotide polymorphisms (SNPs) in the same haploblock are inherited together, a non-functional SNP can be identified statistically as an eQTL if it is located in the same haploblock with a functional eQTL. As there was only one H3K27ac peak in the promoter region of *LACC1* in naïve CD4+ T cells (Fig. 1a), as well as the other lymphoid cells tested, we hypothesized that the functional eQTLs in T cells, linked tightly with rs9567293 in the same haploblock, were in the promoter region.

Using a previously published DICE dataset[17], we identified four sites in the *LACC1* promoter region in high LD with rs9567293 (Fig. 1b–c). Therefore, these sites in the same haploblock could also be T cell specific eQTLs and Crohn's disease risk SNPs. In fact, eQTLs A (rs12868462) and B (rs3816311) were included in a previous analysis and shown to be Crohn's disease risk SNPs[8]. There are multiple transcripts of the *LACC1* gene, but in the most prevalent transcript (ENST00000325686) sites A and B are in the 5' flanking region and C and D are in intron 1. In the other transcript (ENST00000441843), the eQTLs A and B are in the 5' UTR in exon 1 (Fig. 1b). As for the rs9567293 variant, the promoter region sites are in LD with the rs3764147 structural region variant, but because they are more frequent, they also are not highly correlated, as indicated by the r^2 value (Supplementary Table 1). The disease risk promoter region variants are frequent in different ethnic groups (Supplementary Table 2). There is the most variability in the frequency of rs12868462-C, however, reducing the

Promoter eQTLs	SNP	Ref -> Alt	Ref -> Alt (reverse strand)	Disease-risk allele	Location	Linkage disequilibrium (D') with rs9567293	Linkage disequilibrium (r²) with rs9567293
A	rs12868462	C -> T	G -> A	C	5' flanking	-0.99	0.85
B	rs3816311	G -> A	C -> T	A	5' flanking	0.98	0.95
C	rs3215973	AG-> A	CT -> T	A	Intronic	0.96	0.9
D	rs2275252	A -> C	T -> G	C	Intronic	0.96	0.92
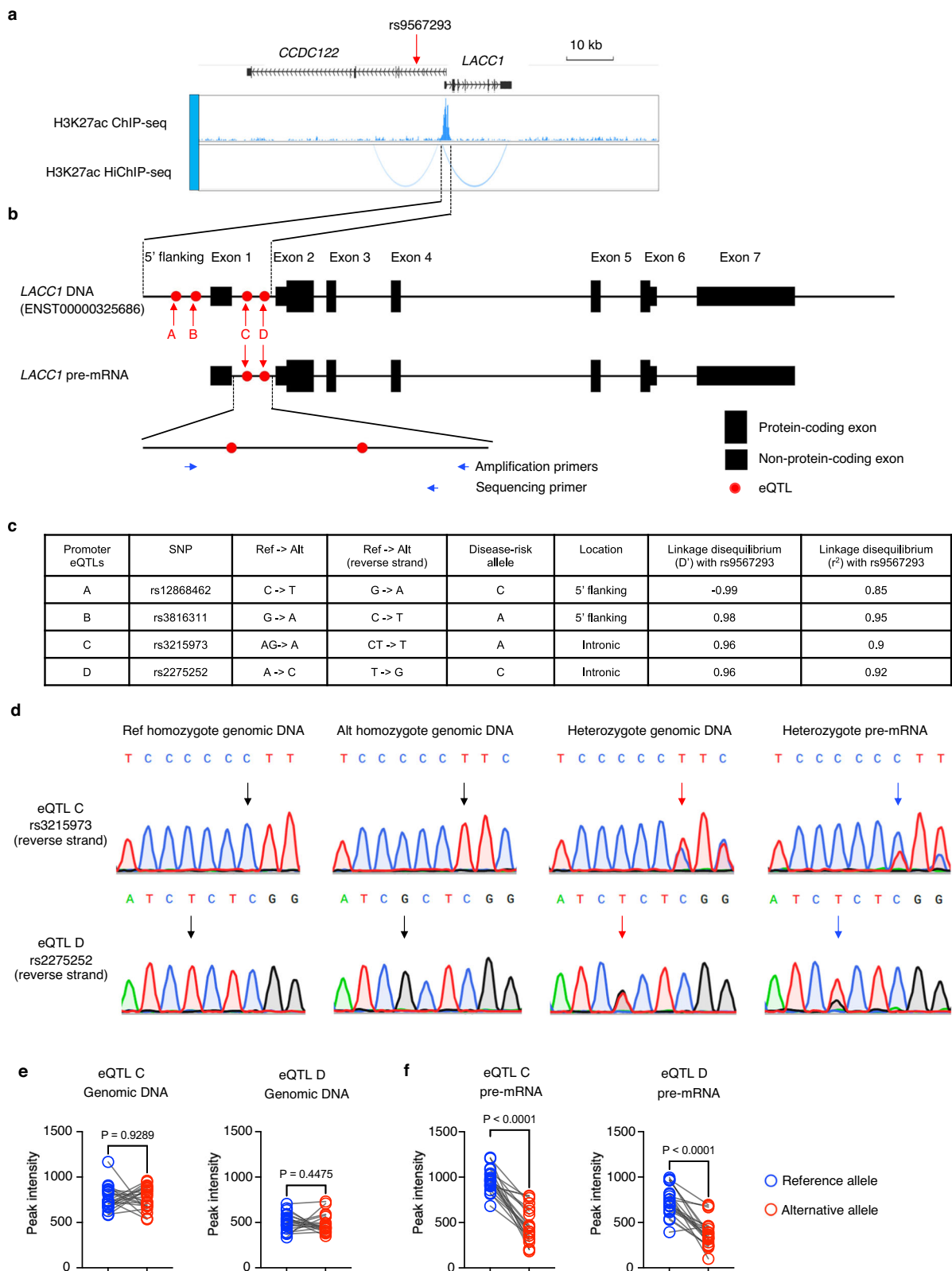
linkage to rs9567293 (Supplementary Table 3). Therefore, as for any GWAS study, the strength of the conclusions may depend on the ethnic group that is analyzed.

The earlier analysis of *LACC1* expression in populations suggested that the disease risk allele caused decreased gene expression, but to confirm this while eliminating other genotypic differences, we compared *LACC1* transcripts derived from the reference and alternative

alleles from naïve, CD4^{+} T cells from heterozygous human donors (rs9567293[T/C]). The cell purity we obtained was as shown in Supplementary Fig. 1e. We activated the cells to increase the transcription of *LACC1*[17]. Given that two eQTLs (eQTLs C & D) are located in the intronic region of all the transcript versions, quantification of transcripts from each allele was achieved by reverse transcription of the pre-mRNA and Sanger sequencing of the intronic region from the reverse direction

Fig. 1 | Promoter eQTLs of *LACC1* are associated with differential gene expression in human CD4⁺ T cells. a WashU Epigenome browser tracks for the extended *LACC1* locus, H3K27ac ChIP-seq tracks (peaks) and HiChIP interactions (curved lines) in human naïve CD4⁺ T cells. Primary data were analyzed from a previous publication[25]. **b** Scheme for analyzing pre-mRNA ratios from each allele from heterozygous CD4⁺ T cells. RNA was extracted from naïve CD4⁺ T cells that were activated prior to reverse transcription, amplification and Sanger sequencing. **c** Four common polymorphisms in the *LACC1* promoter region. **d** Sanger sequencing of homozygous and heterozygous genomic DNA and heterozygous pre-mRNA. Upper: eQTL C (rs3215973). Bottom: eQTL D (rs2275252). **e** Quantification of genomic DNA by measurement of the peak intensity of eQTL C (rs3215973) and eQTL D (rs2275252) in heterozygous CD4⁺ T cells (*n* = 21). eQTLs were indicated by red arrows in (**d**). **f** Quantification of pre-mRNA by measuring peak intensity of eQTL C (rs3215973) and eQTL D (rs2275252) in heterozygous CD4⁺ T cells (*n* = 21). eQTLs were indicated by blue arrows in (**d**). **e**–**f** Each symbol represents an individual human donor. *$p < 0.05$ by Student's paired two-tailed t test.

(Fig. 1b−d). As expected, analyzing genomic DNA, in every donor tested both alleles were equally represented (Fig. 1d-e). The pre-mRNA, however, had decreased transcripts from the alternative or disease-risk allele in each of 21 donors tested (Fig. 1d, f), directly confirming that the disease-risk eQTLs are associated with lower pre-mRNA transcription or accumulation. Therefore, given the previous population level data[17] indicating that the common polymorphisms linked to disease affect gene expression in lymphocytes and not in myeloid cells, and the current data directly implicating an allele-specific effect in heterozygous individuals on gene expression in CD4⁺ T cells, we confirmed that the *LACC1* promoter region has eQTLs that affect gene expression in CD4⁺ T cells. Hence, we carried out a further analysis of the control of gene expression in these cells.

Promoter regions sequences are associated with reduced *LACC1* expression

We tested which of the eQTLs in the promoter region of *LACC1* influenced gene expression. We isolated naïve CD4⁺ T cells from reference allele homozygous human PBMCs and targeted the reference eQTLs using CRISPR Cas9 editing. We quantified *LACC1* mature mRNA expression in targeted and control cells (Fig. 2a). We designed guide RNAs targeting the eQTL flanking sequences for eQTL A (Fig. 2b) and eQTLs B-D (Supplementary Fig. 2a−c). Sanger sequencing confirmed the cutting efficiency for each of the four eQTL sites (Fig. 2c). TF binding sites are typically approximately 10 nucleotides in length[26], therefore random repair at close flanking nucleotides should still have interrupted TF binding and consequently reduced gene expression. On the contrary, changed sequences near non-functional eQTLs should not alter gene expression. Quantitative PCR showed that targeting the promoter region eQTLs A or B reduced *LACC1* mRNA expression in different donors, while targeting the intronic C and D regions did not have a consistent effect comparing different donors (Fig. 2d). In conclusion, we found the more 5′ sites A and B in the promoter region of *LACC1* identified the areas containing the functional *LACC1* eQTLs in CD4⁺ T cells.

Limited influence of LACC1 in mouse colitis

It has been reported that *Lacc1* deficiency in mouse macrophages caused increased inflammation after bacterial infection, increased experimentally induced colitis, and increased arthritis in two models[9,19,21,22,27]. To validate function of LACC1 in mouse myeloid cells, we differentiated bone marrow derived macrophages (BMDM) from *Lacc1⁻/⁻* mice and measured their cytokine production upon LPS stimulation (Supplementary Fig. 3a). The *Lacc1⁻/⁻* BMDM, showed augmented inflammatory cytokines compared to *Lacc1⁺/⁺* and *Lacc1⁺/⁻* BMDM, including a significant increase in IL-12p40 and a tendency to increased TNF and IL-6. The magnitude of the increases were similar to a previous study[19]. We analyzed T cells from *Lacc1⁻/⁻* mice in an attempt to gain mechanistic insights into how reduced LACC1 in T cells might contribute to colitis. In human CD4⁺ T cells *LACC1* expression increased 10-fold upon TCR stimulation[17], however, the expression of *Lacc1* in mouse naïve splenic CD4⁺ T cells remained unchanged after anti-CD3/CD28 stimulation (Supplementary Fig. 3b). At steady-state, there were no *Lacc1*-dependent gross alterations in T lymphocytes in the spleen. Splenic T cells from *Lacc1⁺/⁺*, *Lacc1⁺/⁻*, and *Lacc1⁻/⁻* mice,

gated as in (Supplementary Fig. 3c), had similar numbers of CD4⁺ and CD8⁺ T cells, Foxp3⁺ regulatory T cells (Treg), CD62L⁺CD44⁻ naïve and CD62L⁻CD44⁺ antigen-experienced populations (Supplementary Fig. 3d). The capacity for cytokine production after PMA/Ionomycin stimulation also was not affected (Supplementary Fig. 3e−f). To explore the potential role of T cell expression of LACC1 in experimentally induced colitis, we adoptively transferred naïve CD4⁺CD45RB^high^CD25⁻ mouse T cells (gated as in Supplementary Fig. 4a) from different *Lacc1* genotypes into *Rag1⁻/⁻* mice. As expected, the recipient *Rag1⁻/⁻* mice showed symptoms of colitis, such as diarrhea and a hunched back. Weight loss (Fig. 3a) and colitis histology scores in recipients (Fig. 3b−c, Supplementary Table 4) did not show a *Lacc1* genotype-dependent difference. A small percentage of the transferred CD4⁺CD45RB^high^CD25⁻ mouse T cells converted to Treg in the *Rag1⁻/⁻* mice. In mice that received *Lacc1⁻/⁻* T cells, there was a tendency to a reduction in the induced Treg in mesenteric lymph node (mLN) (Supplementary Fig. 4b), although this difference was not large enough to influence disease course. We also tested the role of LACC1 in DSS-induced colitis, which is influenced by the adaptive immune response[28], although it can be induced in *Rag* deficient mice[29]. We did not observe any LACC1-dependent difference in disease severity in the DSS acute colitis model (Fig. 3d−f, Supplementary Table 4). To test for a LACC1 effect on mouse Treg, we co-transferred wildtype, naïve CD4⁺CD45RB^high^CD25⁻ T cells into *Rag1⁻/⁻* mice with a CD4⁺CD45RB^low^CD25⁺ population enriched for Treg obtained from strains with the different *Lacc1* genotypes (gated as in Supplementary Fig. 4c). With the presence of Treg, colitis development was much slower, with 20% body weight loss reached only after 13 weeks (Fig. 3g). The in vivo suppressive capacity of the donor *Lacc1⁻/⁻* Treg, however, was not significantly diminished as measured by tissue inflammation (Fig. 3h−i). The splenic Treg cells in the co-transfer were predominantly natural or thymus Treg, and therefore we also investigated if *Lacc1* deficiency influenced Treg induction, as suggested by the reduced conversion in vivo after cell transfer (Supplementary Fig. 4b). We differentiated Treg cells in vitro with TGF-β and IL-2. *Lacc1⁺/⁻* and *Lacc1⁻/⁻* T cells showed significantly lower induced Treg differentiation, compared to *Lacc1⁺/⁺* T cells (Fig. 3j). In summary, analyzing mice on the C57BL/6 genetic background, we did not obtain evidence that *Lacc1* gene deficiency affected CD4⁺ T cell-induced colitis pathogenesis following transfer to *Rag1⁻/⁻* mice, with no effect on spontaneous colitis, colitis induced by chemical injury in mice with a whole-body deficiency for *Lacc1*, colitis caused by transfer of CD4⁺ T cells, or natural Treg differentiation or function. The differentiation of iTreg in vitro was impaired by *Lacc1* deficiency, although it was not sufficiently altered in vivo to affect disease severity in our experimental systems.

Knocking down *LACC1* in human CD4⁺ T cells

The regulation of *LACC1* gene expression in mouse compared to human CD4⁺ T lymphocytes differs, and perhaps as a consequence, LACC1 function in mouse and human T lymphocytes also may differ. Therefore, to explore the basis for the GWAS-discovered genetic risk for CD, we concentrated on the role of LACC1 in human CD4⁺ T cells. To eliminate differences in genes other than *LACC1*, we knocked down *LACC1* using a lentiviral shRNA system in CD4⁺ T cells from different individuals and compared the knockdown cells to the empty vector
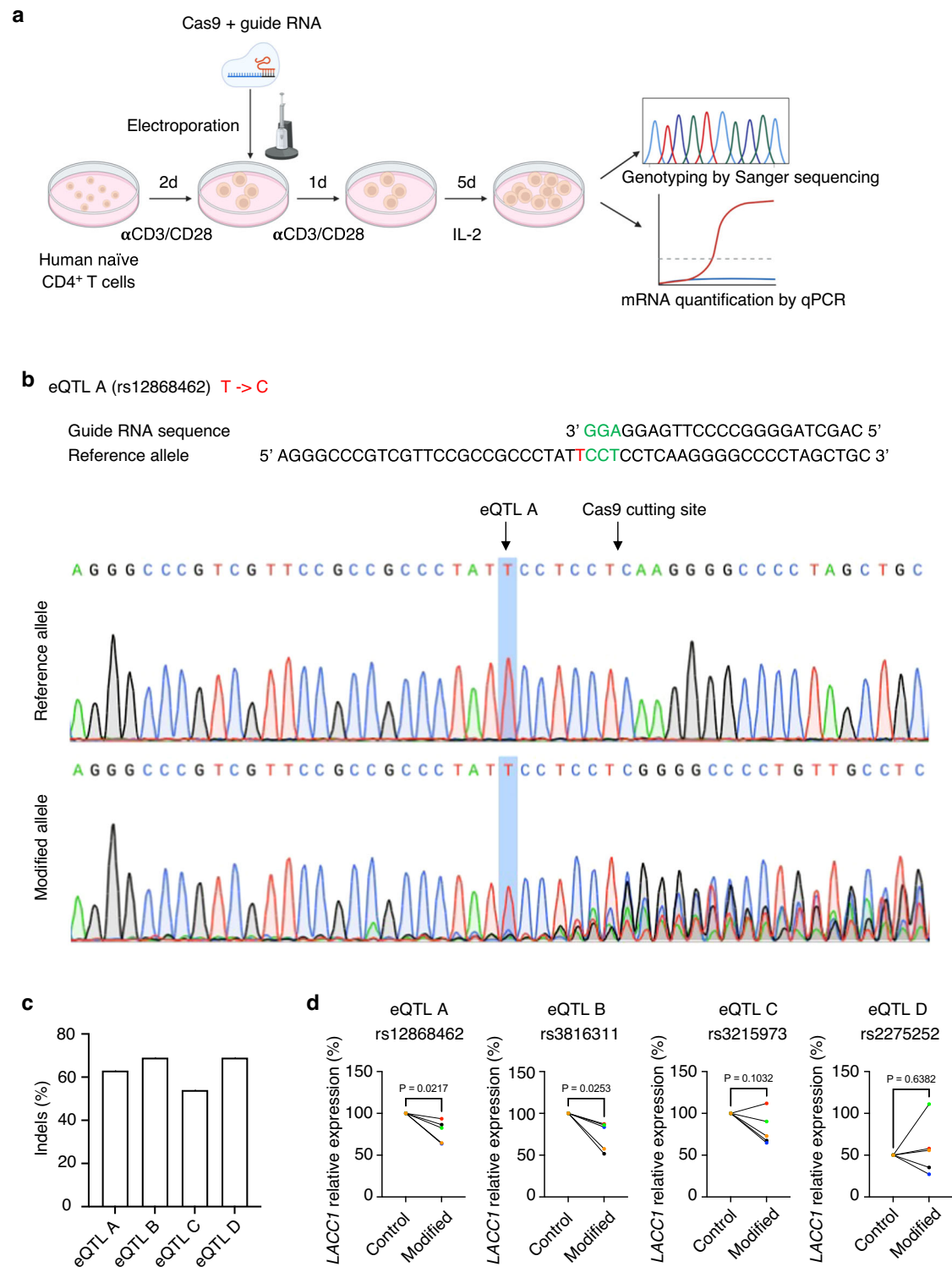
Fig. 2 | Functional promoter eQTLs determined by gene editing. a Scheme of CRISPR Cas9-mediated editing in human naïve CD4+ T cells that were activated. Graph was created in BioRender. Chou, T. (2025) https://BioRender.com/g28z114. **b** Guide RNA design (upper panel); green letters indicate PAM sequence; red letter indicates nucleotide defining the eQTL. The Sanger sequencing result of the non-edited reference and CRISPR Cas9 modified alleles (bottom panel) of eQTL A (rs12868462). Arrows indicate the eQTL and Cas9 cutting sites. **c** Percentage of indels of the four eQTLs after editing. Indels were calculated by the substitution rate of the nucleotide downstream of the Cas9 cutting site; for example, the nucleotide C directly downstream of the Cas9 cutting site in (**b**). **d** Quantification of *LACC1* mRNA of T cells post editing (*n* = 5, superposition makes it difficult to see some subjects). **d** Each symbol represents an individual human donor. *p < 0.05 by Student's paired two-tailed t test. Representative data from one of several experiments in which 3–5 donors were tested at a time.

a Donor cells:
- *Lacc1*+/+ naïve CD4 T cells (*n* = 9)
- *Lacc1*+/- naïve CD4 T cells (*n* = 8)
- *Lacc1*-/- naïve CD4 T cells (*n* = 8)
- Mock (*n* = 3)

d
- *Lacc1*+/+ (*n* = 6)
- *Lacc1*+/- (*n* = 8)
- *Lacc1*-/- (*n* = 5)

g Donor cells:
- Naïve CD4 + *Lacc1*+/+ Treg cells (*n* = 5)
- Naïve CD4 + *Lacc1*+/- Treg cells (*n* = 3)
- Naïve CD4 + *Lacc1*-/- Treg cells (*n* = 5)
- Mock (*n* = 1)
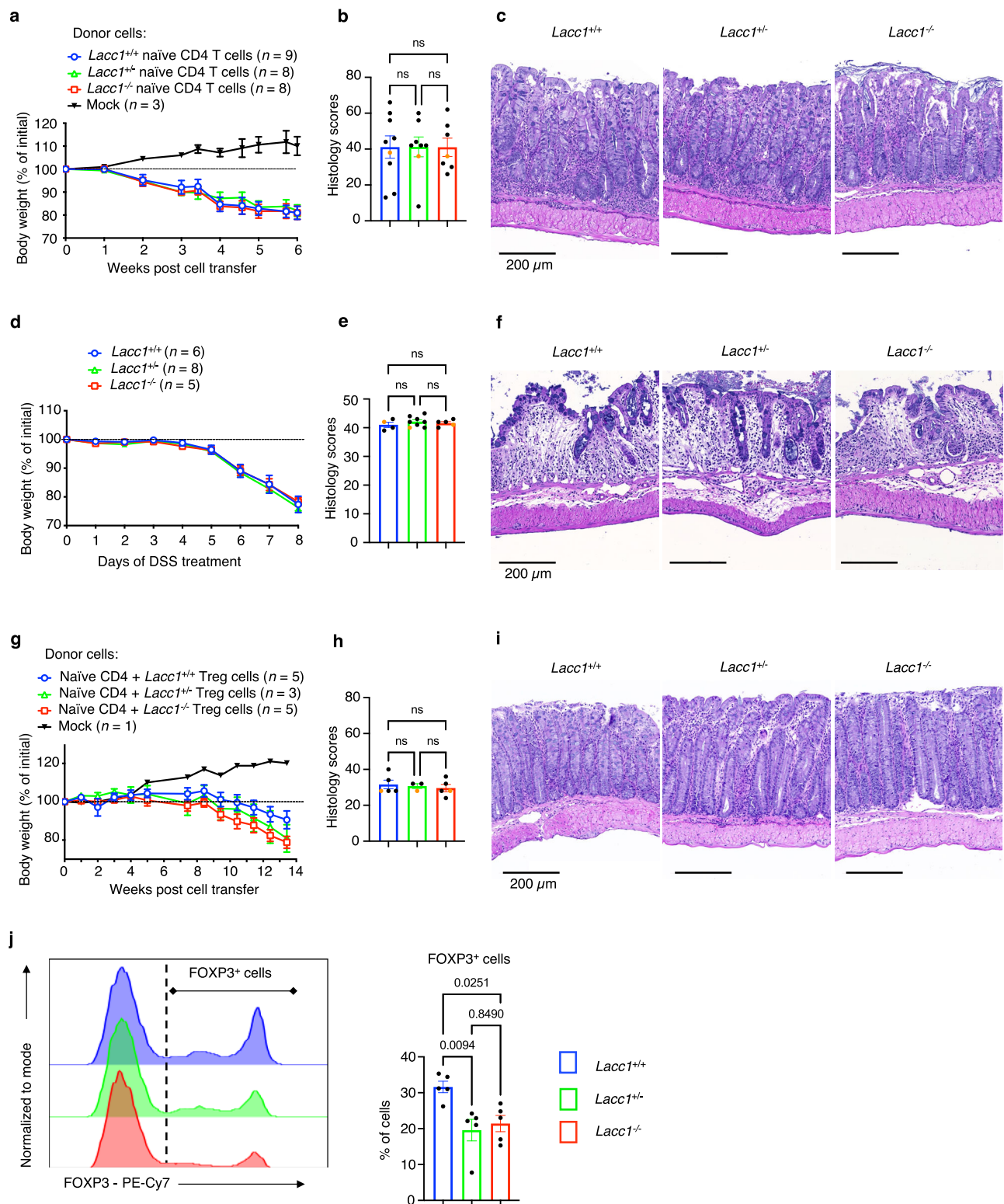
j
FOXP3+ cells
- *Lacc1*+/+
- *Lacc1*+/-
- *Lacc1*-/-

controls from the same individual. Unlike the rare *LACC1* missense mutations described above, the great majority of individuals homozygous for the disease risk alleles do not have early-onset inflammatory disease. Therefore, a decrease in *LACC1* gene expression, as opposed to knocking out the gene, might be more reflective of subjects who carry a disease-risk allele. To reduce *LACC1* expression, naïve human CD4+ T cells were stimulated with anti-CD3/CD28 and transduced with lentivirus (Fig. 4a). After culture in IL-2 inducing cell division, Th0 conditions, more than 80% of the resulting CD4+ T cells showed GFP

reporter expression (Supplementary Fig. 5a), indicative of a high transduction efficiency. Compared to empty vector (EV) controls, in cells harboring a targeted shRNA, *LACC1* mRNA expression in multiple donors was reduced by approximately 80% (Supplementary Fig. 5b). LACC1 protein expression also was reduced, by 20–80% (Supplementary Fig. 5c–d). Although oxygen consumption was increased by EV vector transduction of human CD4+ T cells (Supplementary Fig. 5e), however, cells treated in this way provide the best control to vector-mediated *LACC1* knock down.

Fig. 3 | *Lacc1* deficiency does not affect colitis in mice but reduced T reg induction. a–**c** Adoptive T cell transfer model of colitis. Splenic CD4⁺CD45RB^high^CD25⁻ T cells from donor mice were adoptively transferred into *Rag1*⁻/⁻ mice. **a** Body weight measurement of *Rag1*⁻/⁻ mice post T cell transfer (*Lacc1*⁺/⁺ n = 9; *Lacc1*⁺/⁻ n = 8; *Lacc1*⁻/⁻ n = 8). **b** Histology scores of the colon tissues (*Lacc1*⁺/⁺ n = 9; *Lacc1*⁺/⁻ n = 8; *Lacc1*⁻/⁻ n = 7). **c**, Representative images (orange dots in **b**) of hematoxylin and eosin (H&E) stained tissues. **d**–**f** DSS oral feeding model of colitis. Mice were fed with 2.5% DSS water. **d** Body weight measurement of mice (*Lacc1*⁺/⁺ n = 6; *Lacc1*⁺/⁻ n = 8; *Lacc1*⁻/⁻ n = 5). **e** Histology scores of the colon tissues (*Lacc1*⁺/⁺ n = 4; *Lacc1*⁺/⁻ n = 8; *Lacc1*⁻/⁻ n = 5). **f** Representative images (orange dots in **e**) of the H&E histology. **g**–**i** Adoptive T cell transfer model of colitis. CD4⁺CD45RB^high^CD25⁻ WT T cell and Treg cells from the indicated *Lacc1* genotypes were adoptively co-transferred into *Rag1*⁻/⁻ mice. **g** Body weight measurement of *Rag1*⁻/⁻ mice post T cell transfer (*Lacc1*⁺/⁺ n = 5; *Lacc1*⁺/⁻ n = 3; *Lacc1*⁻/⁻ n = 5). **h** Histology scores of the colon tissues (*Lacc1*⁺/⁺ n = 5; *Lacc1*⁺/⁻ n = 3; *Lacc1*⁻/⁻ n = 5). **i** Representative images (orange dots in **h**) of the H&E histology. **j** Analysis of Treg in vitro differentiation. Mouse splenic naïve CD4⁺ T cells (n = 5 for each group) were cultured in Treg induction culture conditions. (**a, d, g**) Data of body weight plots are mean +/− SEM and statistical significance for comparisons was computed using two-way ANOVA and adjustments were made for multiple comparisons. (**b, e, h, j**) In the representation of histology data, each symbol represents an individual mouse. Small horizontal lines indicate the mean (± SEM). Statistical significance for comparisons was computed using one-way ANOVA and adjustments were made for multiple comparisons. Each experiment was repeated at least two times.

To gain insight into the metabolic processes affected by decreased LACC1 expression, we performed bulk RNA sequencing of human CD4⁺, *LACC1* knockdown (KD) Th0 cells and controls. The differentially expressed genes in the *LACC1* knockdown (KD) Th0 cells are shown in Supplementary Fig. 5f and Supplementary Data 1. We analyzed for changes in the expression of genes related to metabolism through Gene Set Enrichment Analysis (GSEA). In this analysis, one of the highly scored, negatively regulated gene sets in the *LACC1* KD cells was fatty acid metabolism (Fig. 4b). This is consistent with the previous finding of downregulated fatty acid and lipid metabolism in *Lacc1*⁻/⁻ macrophages[5,9].

LACC1 influences metabolism in human CD4⁺ T cells

We tested mitochondrial activity in *LACC1* KD CD4⁺ T cells by flux analysis in the Seahorse instrument using the Mito Stress assay for determination of oxygen consumption rates (OCR). *LACC1* KD CD4⁺ T cells showed a lower OCR than the EV controls at the basal respiration level (Fig. 4c), indicating lower energy demand. The KD cells also had lower maximal respiration and spare respiratory capacity (Fig. 4c), indicative of decreased mitochondrial functionality. These changes align with the previous findings in macrophages from *Lacc1*⁻/⁻ mice[5,9]. Glycolytic rate was also previously found to be reduced in *Lacc1*⁻/⁻ macrophages[5]. Mildly reduced glycolytic reserve was evident in the KD T cells in the glycolysis stress test assay, while we did not detect striking changes in glycolysis rate or capacity (Fig. 4d).

To further investigate the metabolic pathways that were altered in human CD4⁺ T lymphocytes with reduced LACC1 protein expression, we traced metabolites by adding carbon-13 (¹³C) glucose in the culture medium followed by detection of metabolites through liquid chromatography-mass spectrometry (LC-MS) (Supplementary Fig. 5g). The majority of significantly affected metabolites in negative mode datasets occurred in the glycolysis, pentose phosphate pathway (PPP) and purine metabolic pathways (Fig. 4e, Supplementary Fig. 5h, **top**). Early glycolytic metabolites glucose-6-phosphate (G6P) and glucose-1-phosphate were decreased, while downstream glyceraldehyde 3-phosphate (GAP), and fructose 1,6-bisphosphate (F1,6BP) were increased, perhaps consistent with activation of the pentose phosphate shunt (Fig. 4e). Gluconate-6-phospate, an intermediate in the PPP, showed reduction in the *LACC1 KD* cells, while the purine metabolites XMP, IMP and GMP were all increased in the *LACC1* KD cells (Fig. 4e). These data are consistent with the reported role of LACC1 as a purine metabolic regulator in macrophages[18]. In the positive ion mode (Supplementary Fig. 5h, **bottom**), carbamoylaspartate, a metabolite in the mitochondrial shuttle system, showed a mild decrease. Therefore, combining the RNA-seq and metabolomic data, we conclude that *LACC1* knockdown resulted in increased expression of genes related to inflammatory processes and changed metabolic programming in human CD4⁺ T cells.

LACC1 Knockdown alters T cell function

To test the functional effect of reduced LACC1 expression, we measured T cell proliferation with CellTrace Violet (CTV). *LACC1* KD cells showed lower CTV mean fluorescence intensity (MFI) (Supplementary Fig. 6a), indicating that the naïve CD4⁺ T cells that were cultured were more proliferative. T cell subsets adopt different metabolic pathways to support their distinct functions[30]. For example, Th1 and Th17 cells preferentially use aerobic glycolysis for energy supply and largely depend on the mTORC1 pathway, while T regulatory cells skew to lipid metabolism and they have low mTORC1 function, but high AMPK activity[30]. Therefore, to understand how T cell subset formation is affected by reduced LACC1 expression and accompanying metabolic changes, we polarized human naïve CD4⁺ T cells into different T helper cell subsets during in vitro culture. We induced IL-2 producing cells in Th0 culture conditions (Supplementary Fig. 6b), and IFNγ-expressing Th1 cells in cultures containing IL-12 (Supplementary Fig. 6c). IL-17A producing T cells were cultured in a cytokine cocktail containing IL-1β, TGFβ and IL-23 (Supplementary Fig. 6d). *LACC1* KD and control EV CD4⁺ T cells did not show a difference for in vitro IL-2, Th1- or Th17 cell-related cytokine secretion, although only few CD4⁺ T cells could be induced to produce IL-17A.

In agreement with our earlier findings[17], in the Th0 condition IL-2 receptor α chain (CD25) expression was significantly decreased in the *LACC1* KD CD4⁺ T cells after anti-CD3/CD28 stimulation (Fig. 5a). Consequently, we tested Treg cell differentiation which depends on CD25. To induce Treg, we cultured CD4⁺ T cells in IL-2 with different concentrations of TGFβ. The expression of the Treg signature transcription factor FOXP3 showed a dose-dependent increase with increasing TGFβ in different human donors (Supplementary Fig. 6e). There consistently was reduced FOXP3 induction in the *LACC1* KD group, however, which was most evident at the 5 ng/mL TGF-β concentration (Fig. 5b), suggesting that decreased LACC1 expression impaired Treg cell differentiation in vitro. To examine the suppressive function of CD4⁺ T cells, we quantified the expression of IL-10 by intracellular staining after PMA/Ionomycin treatment. The intracellular expression of IL-10 also showed a TGF-β dose-dependent increase (Supplementary Fig. 6f), with a reduction in the *LACC1* KD total CD4⁺ T cells (Fig. 5c) and specifically in the cells that induced FOXP3⁺ expression (Supplementary Fig. 6g).

In a transcriptomic analysis of the cells in the induced Treg culture, the *LACC1* KD cells showed a reduction in the Treg gene signature (Fig. 5d, Supplementary Data 2). Affected Treg-related genes included *FOXO3*, absence of which exacerbated the Treg-related autoimmunity due to the loss of Foxo1 expression in mouse Treg[31,32] (Fig. 5e). Also decreased in the *LACC1* KD Treg cell cultures (Fig. 5e) was Melanoma antigen family H1 gene (*MAGEH1*), which is increased in intratumoral Treg and might function to support Treg cell survival in tumors[33]. ICOS ligand (*ICOSLG*) has higher expression in Treg compared to other T cells[17], was also decreased *LACC1* KD Treg cells. Mouse Treg have higher AMPK activity[34], and p38 AMPK signaling is required for mouse iTreg cell differentiation[35]. Therefore, we analyzed the expression of genes in the AMPK pathway and we found that expression of *MAPK11*, which encodes p38β kinase, was significantly decreased in *LACC1* KD Treg cells (Fig. 5e). To test the suppression function of these induced Treg cells, we co-cultured them with CD4⁺ T effector cells, which were
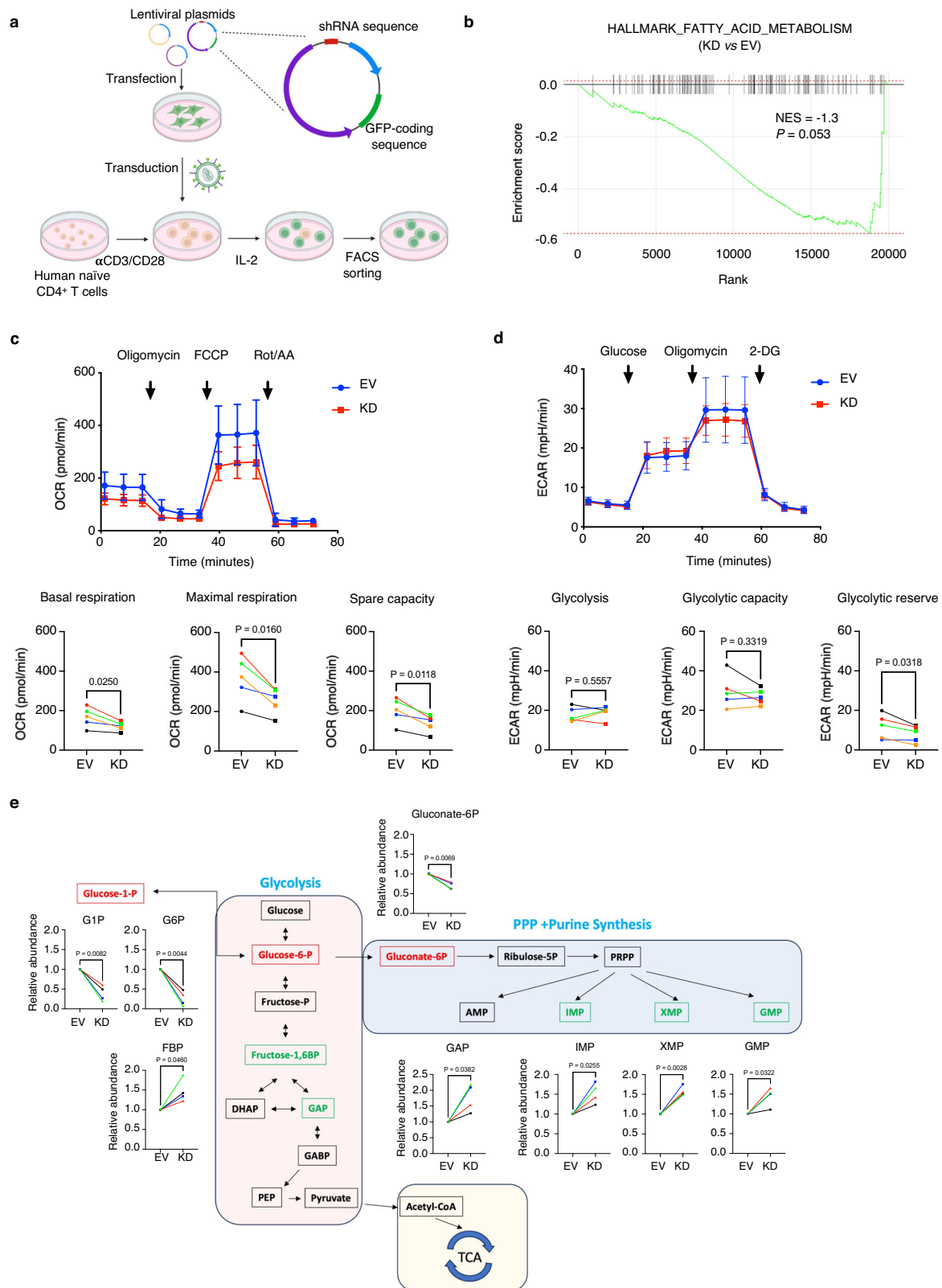
generated by activating naïve CD4^{+} T cells with anti-CD3. CD4^{+} T effector cells co-cultured with *LACC1* KD Treg cells showed slightly higher proliferation at different Treg: T effector ratios (Figs. 5f and Supplementary Fig. 6h), indicating weaker suppressive function of the *LACC1* KD Treg cells. Overall, decreased *LACC1* expression led to changes that could contribute to increased colitis risk including increased naïve T cell proliferation in vitro, reduced the transcription of genes related to Treg induction or function, and impaired Treg differentiation in vitro accompanied by decreased IL-10 synthesis and weaker suppressive function.

Discussion

In this study, we focused on understanding the mechanism how a GWAS hit based on a common variant in a noncoding region near the

Fig. 4 | LACC1 is a metabolic regulator in human CD4+ T cells. a Scheme of *LACC1* knockdown by lentiviral transduction in human naïve CD4+ T cells. Graph was created in BioRender. Chou, T. (2025) https://BioRender.com/i90h862.
b−**c** Transcriptomic analysis of CD4+ Th0 cells post viral transduction with empty vector (EV) and *shLACC1* (KD), 5 donors were tested individually. Bulk RNA sequencing was conducted on the cells. **b** Gene set enrichment analysis (GSEA) based on differentially expressed genes, considering significantly different genes with an absolute log$_2$ Fold-Change higher than 1 and adjusted *p*-value less than 0.05 (*n* = 5). **c** Oxygen consumption rate (OCR) of human CD4+ Th0 cells post viral transduction with empty vector (EV) and *shLACC1* (KD) (*n* = 5). For each donor, 3–5

technical replicates were tested, 2×10^5 cells were tested for each technical replicate. **d** Extracellular acidification rate (ECAR) of human CD4+ Th0 cells post viral transduction with EV and KD (*n* = 5). For each donor, 3-5 technical replicates were tested, 2×10^5 cells were tested for each technical replicate. **e** Metabolite levels of human CD4+ Th0 cells post viral transduction with EV or *Lacc1* KD (*n* = 4). In each donor, the relative abundance of each metabolite was normalized to the EV. **c**−**d** Top OCR and ECAR plots, small horizontal lines indicate the mean (± SEM) of 5 donors. Bottom, each symbol represents the average of technical replicates of an individual human donor. **e** Each symbol represents an individual human donor. **p* < 0.05 by Student's paired two-tailed t test.

LACC1 gene contributed to the genetic risk for IBD. GWAS have implicated genetic variants for many human diseases, however, the cell types and genes affected, and the mechanisms of action of the variants, are in most cases unknown. To address the question in immune cells, the DICE project was launched, and in the first report, it defined eQTLs in 13 immune cell types[17]. A surprising finding was that many of them are cell-type specific[17]. In the second report, DICE identified eQTLs that overlap active *cis*-regulatory elements in five immune cell types, including some eQTLs that interact with their target gene promoters (promoter-interacting eQTLs or pieQTLs)[25]. These data provided insights into possible molecular mechanisms eQTL regulation of gene expression in a cell-type specific manner.

GWAS studies implicate several other genes in the genomic region flanking *LACC1* associated with Crohn's disease (CD)[1,2,6,7] and ulcerative colitis (UC)[8], with fine mapping more strongly implicating the risk for CD[36]. The genes in this region include *ENOX1*, *LINC00284* and *CCDC122*. However, *ENOX1* and *LINC00284* are not expressed in human immune cells according to the DICE database[17]. While the expression of *CCDC122* was associated with CD-risk variants, its expression was low in immune cells (Mean TPM < 2). Therefore, although our study does not rule out an effect of CD-risk variants on the expression of these genes in other cell types, we focused on *LACC1* as an excellent target for obtaining a deeper understanding of eQTL action in immune cells, because rare missense mutations that eliminate function confirm that it is relevant for causing inflammatory diseases, including IBD and juvenile idiopathic arthritis[1,2,7]. Furthermore, the starting point for this study, rs9567293, is typical of many findings from GWAS, because it imparts only a mild increased risk, the rs9567293$^{C/C}$ risk genotype is common in healthy people too, and it is embedded in a haploblock. Despite higher expression and much evidence for LACC1 function in macrophages, our previous data suggest that a GWAS hit associated Crohn's disease is an eQTL lymphocytes[17], therefore we concentrated on CD4+ T cells to understand how common variants in this locus affected IBD pathogenesis. We began this investigation with the notion that the relevance of LACC1 for disease pathogenesis was not in question, but how it acts in lymphocytes, a cell type demonstrating an eQTL for this gene, remained unknown. We note that rs3764147, the V254I substitution in LACC1 that decreases LACC1 metabolic activity and also is implicated in IBD causation, will act in every cell type where the protein is expressed. Furthermore, it is in linkage disequilibrium with the promoter eQTLs, but because it is less frequent, the r^2 value is not high. This structural change does not affect steady state protein[5,9]. Therefore the promoter region variants provide a separate and more common genetic contribution to LACC1 expression and perhaps IBD causation that acts in CD4+ T cells and other lymphocytes. Our study did not measure the separate contributions of rs9567293 and rs3764147 on disease risk at the population level in CD patients, or in T cells by separate CRISPR mutations followed by in vitro functional studies. Our interpretation, however, based on the previous data and combined with our functional studies of T cells with *LACC1* expression knocked down, is that both contribute to risk. Further analyzes would be required to quantify the relative contributions of the different genotypes.

Our previous population-level data associates lower expression of *LACC1* with IBD risk[17]. Here, by analyzing multiple heterozygous individuals, we demonstrated that the risk allele caused decreased *LACC1* RNA expression in CD4+ T cells. Despite this, rs9567293 itself did not show histone marks indicative of an active enhancer nor interactions with an enhancer region in naïve CD4+ T cells by HiChIP. Within the haploblock, however, we showed that two eQTLs, A (rs12868462) and B (rs3816311), mark functional eQTLs in CD4+ T cells using CRISPR-based gene editing. These are in the area that contains the promoter, -500 bp from the transcription start site of the major transcript ENST00000325686. We conclude that *LACC1* transcription was most likely affected by the functional eQTLs in the promoter region, but it remains to be determined how these sites affected the amount of *LACC1* RNA or if they affect LACC1 protein expression.

Importantly, our data do not exclude or contradict a role for decreased LACC1 in macrophages or other cell types as a contributing factor to IBD pathogenesis in some patients. Doubtless that mutations in the *LACC1* coding sequence disrupting function or creating a hypomorphic allele will have effects in all cell types where LACC1 is expressed. Although the functional results of decreased LACC1 in macrophages differ in the published studies, given the consistent reports of altered macrophage function[5,9,19,21], it is reasonable that decreased LACC1 function in macrophages, and perhaps in other myeloid cells such as neutrophils, are important for the etiology of CD and UC. Despite this, the expression analysis of the genetic risk imparted by common variants in the promoter region identified variation in the amount of lymphocyte LACC1 as important for pathogenesis. Furthermore, using gene knockdowns, we showed that the amount of LACC1 affected CD4+ T cell metabolism and function. In this work we concentrated on CD4+ T cells, because the proinflammatory cytokines these cells produce have been implicated in IBD, but important allele-dependent roles for the amount of LACC1 in CD8+ T cells and B cells are also possible.

Mouse models have been important for understanding mechanisms of IBD pathogenesis, and therefore, we explored if decreased LACC1 contributed to pathogenesis in two commonly used mouse models of colitis. We could not confirm the earlier finding that *Lacc1*$^{-/-}$ mice are more susceptible to DSS-induced colitis[22], which is not dependent on T cells, although differences in the microbiome in different colonies can exert a very strong influence on the outcome in this model. Ablation of T cell LACC1 expression did not cause more severe disease when cell transfers of *Lacc1*$^{-/-}$ CD4+ naïve T cells were analyzed. Similarly, the disease-preventive capability of transferred *Lacc1*$^{-/-}$ Treg was not affected. Comparative studies of mouse and humans of disease causation can provide contrasting results for a variety of reasons[37], including differences in gene regulation[38]. The increased expression of *LACC1* in resting and especially in activated human CD4+ T cells compared to their mouse counterparts could be one reason for the lack of an effect of the loss of LACC1 expression on colitis in mice. Another issue is the genetic background of C57BL/6 mice, which might decrease the severity of some colitis models. For example, *Il10*$^{-/-}$ C57BL/6 mice have mild disease compared to *Il10*$^{-/-}$ 129 strain mice[39]. Unlike the infrequent individuals deficient for LACC1 function that present in the clinic, it is striking that *Lacc1*$^{-/-}$ mice analyzed in several
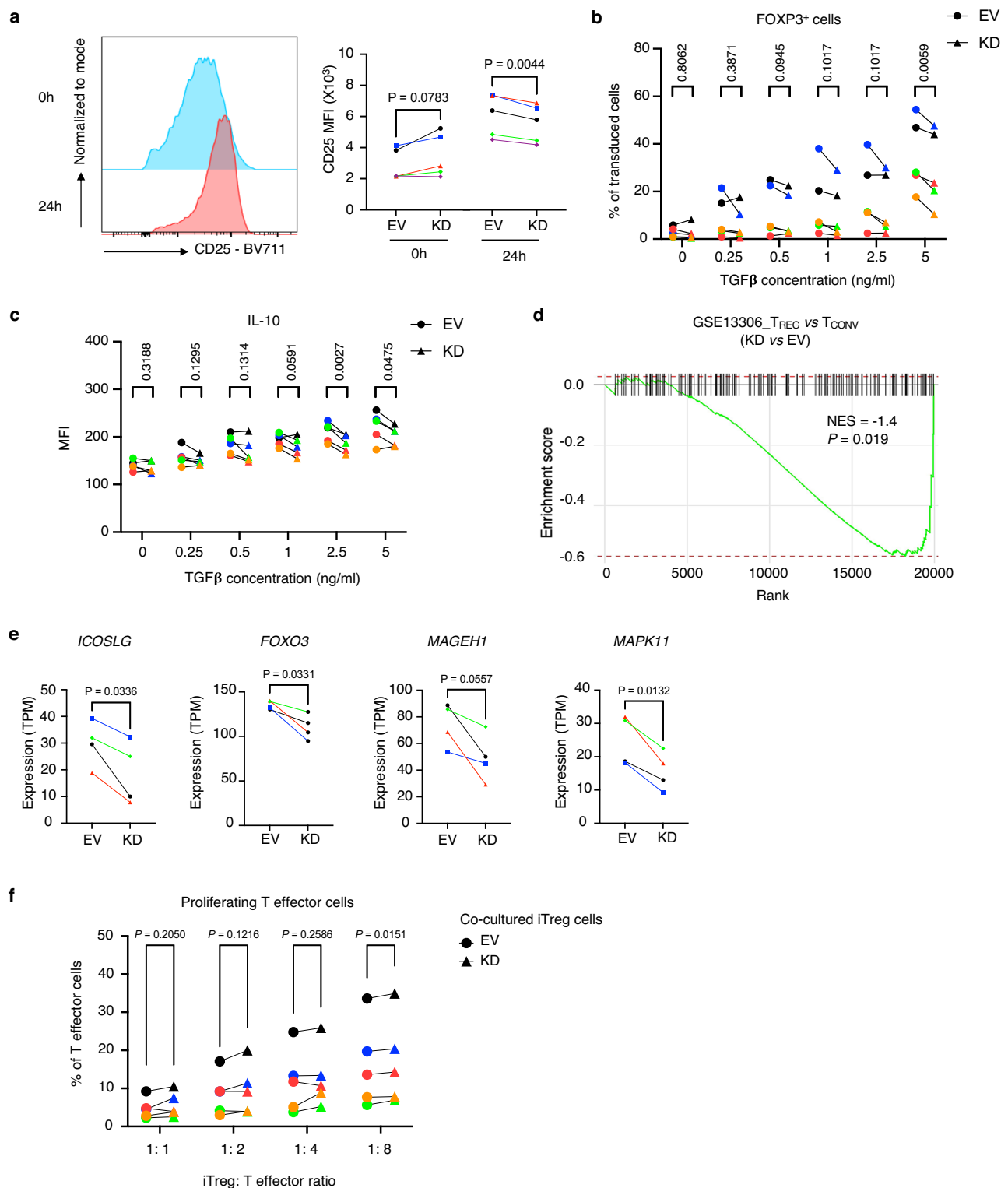
Fig. 5 | Decreased LACC1 impaired human Treg induction in vitro. a Analysis of CD25 expression by human CD4⁺ T cells from different individuals ($n = 5$) that were transduced and cultured in a Th0 condition post anti-CD3/CD28 re-stimulation. Left, representative CD25 staining of CD4⁺ T cells without (blue histogram) and with re-stimulation (red histogram). Right, quantification of the MFI. **b** Analysis of FOXP3 induction. Human naïve CD4⁺ T cells ($n = 5$) were transduced and cultured in Treg induction culture conditions with increasing TGFβ concentrations. **c** Flow cytometric analysis of intracellular IL-10 expression by cells that induced Foxp3 expression in the culture in (**b**) following PMA/Ionomycin treatment. **d** GSEA based on differentially expressed genes of *LACC1* KD cells that induced Foxp3 expression

compared to EV controls, considering significantly different genes with an absolute $\log_2$ Fold-Change higher than 1 and adjusted *p*-value less than 0.05 ($n = 4$). Statistics calculated using MAST. Adjusted *p*-values are Benjamini-Hochberg FDR-corrected *p*-values. **e** Gene expression of Treg-related or inflammation-related genes ($n = 4$). **f** Frequency of proliferating CD4⁺ T effector cells co-cultured with EV or *LACC1* KD iTreg cells. 5×10^4 naïve CD4⁺ T were stained with CellTrace Violet and then co-cultured with transduced iTreg cells at different ratios for 5 days in the culture medium containing soluble anti-CD3 antibody ($n = 5$). (**a–c**, **e**, **f**) Each symbol represents an individual human sample. *$p < 0.05$ and **$p < 0.01$ by Student's paired two-tailed t test.

laboratories do not develop spontaneous colitis or arthritis, although they are more susceptible in several studies of induced disease[5,19,22]. We did observe a significant decrease in Treg induction in vitro when analyzing naïve CD4^{+} T cells from *Lacc1*^{−/−} mice. Although this difference was not sufficient to cause more aggressive colitis, it is consistent with our findings analyzing Treg induction using human CD4^{+} T cells. Overall, considering our findings and other data, the analysis of LACC1 provides an example in which mouse models provide some consistency with data derived from human cells, although they may not reflect differences in human cells related to the genetic basis of pathogenesis of human IBD.

By extracellular flux analysis, OCR was lower in *LACC1* KD CD4^{+} T cells. This result is similar to what had been observed in mouse macrophages[5,9], although unlike in macrophages, ECAR was not strongly decreased. Furthermore, by metabolic tracing, the concentration of intermediates in glycolysis, pentose phosphate pathway (PPP) and purine metabolic pathways were altered, in part consistent with the earlier findings in myeloid cells[5,9,18,19]. Our data do not resolve the controversies surrounding LACC1 function in metabolism from the extensive analyzes that have been done in mouse and human macrophages and transfected cells[5,9,18,19], but they suggest a broad regulatory function of LACC1 in T cell metabolism. In the most recent report, it was shown that LACC1 converts L-citrulline to L-ornithine in mouse macrophages, and the production of proinflammatory cytokines caused by *Lacc1* deficiency was reversed by the presence of L-ornithine[19]. Ornithine is an important metabolic node in both glutamine and arginine catabolic pathways and accumulation of ornithine, caused by inhibition of ornithine decarboxylase, reduced T cell proliferation[40]. It's highly possible that *LACC1* deficiency reduced ornithine production and consequently promoted T cell proliferation, which could potentially explain increased T cell proliferation in human CD4^{+} T cells with *LACC1* knocked down. In addition, inhibition of ornithine decarboxylase enhanced iTreg differentiation[40,41]. Therefore, reduction of mouse and human iTreg differentiation in *LACC1* deficient T cells could also be regulated by reduced ornithine production. We note, however, that alteration in other metabolic pathways reported to be influenced by LACC1 also could be equally relevant.

We also observed changes in T cell function in *LACC1* KD human CD4^{+} T cells. Although the synthesis of cytokines was not decreased after activation of *LACC1* KD CD4^{+} T cells in short term cultures, there was reduced cell surface expression of CD25. This was potentially important, because of the importance of IL-2 signaling and CD25 expression for the generation of induced Treg. Induced or peripheral Treg are prevalent in the intestine in mice and play a role in the prevention of induced colitis[42], and therefore we tested the effect of LACC1 expression on human Treg induction. At higher TGF-β concentrations, the induction of Foxp3 expression was reduced in *LACC1* KD CD4^{+} T cells, and IL-10 expression also was decreased. RNA-seq analysis also suggested decreased Treg induction. These effects on T lymphocyte function provide a plausible link between reduced *LACC1* gene expression, metabolic changes that include reduced oxidative consumption, and changes in function that could contribute to colitis pathogenesis. The magnitude of the effects is consistent with the mildly increased risk of CD in individuals with reduced expression of *LACC1* due to promoter region alterations.

Single gene mutations that lead to early onset IBD have provided important knowledge[10], but are relatively infrequent. In most IBD patients, subtle alterations in groups of genes contribute to disease risk. GWAS provides insights into the gene variants that contribute to disease pathogenesis, but these are mostly not in the coding region and additional research is needed to define the gene and cell type(s) affected. Our findings show that a common variant providing IBD risk that reduces LACC1 acts in CD4^{+} T lymphocytes in the promoter region, to alter aspects of T cell metabolism and Treg function. A limitation of our findings,

and the GWAS studies they are built on, is the degree to which they apply to diverse ethnic groups. For example, African origin populations were not highly represented in the original DICE data set. Regardless, considering the frequency with which eQTLs are restricted to one or a few cell types, the findings illustrate the importance of analyzing well-defined cell types to gain understanding of the genetic basis for pathogenesis of IBD and other autoimmune diseases, as well as careful analysis of different ethnic groups. Analysis of this type in groups of disease risk alleles in affected individuals can provide important information as to the cell types and pathways involved that will provide insights into therapeutic strategies.

Methods

Ethical statement
We have complied with all relevant ethical regulations. All animal work was approved by the La Jolla Institute for Immunology (LJI) Animal Care and Use Committee under protocol no. AP1007. The Institutional Review Board (IRB) of LJI approved the human study under protocol no. SGE-121-0714.

Mice
Lacc1[tm1a(KOMP)/Wtsi] (*Lacc1*^{−/−}; C57BL/6 N) (stock no. 048380-UCD) mice were obtained from the Knockout Mouse Project (KOMP) repository, University of California, Davis. B6.129S7-*Rag1*[tm1Mom]/J (*Rag1*^{−/−}) (stock no. 002216) and C57BL/6 J (stock no. 000664) mice were obtained from the Jackson laboratory. All mice were between 6–14-weeks-old at the beginning of the experiment. All mice were bred and housed under specific pathogen–free conditions in a standard 12-hour light / 12-hour dark cycle at 20 °C and 50% humidity in the vivarium of La Jolla Institute for Immunology. Mice were fed standard rodent chow and water *ad libitum*. All animal work was approved by the La Jolla Institute for Immunology (LJI) Animal Care and Use Committee. In each experiment mice were sex and age matched. Mice of both sexes were used. Sex was not considered in the study design and analysis.

Human samples
Healthy volunteers were recruited in the San Diego area, who provided written, informed consent for collecting leukapheresis samples at the San Diego Blood Bank and sharing deidentified data for research purposes. All donors self-reported ethnicity and race details, and were tested negative for hepatitis B, hepatitis C and human immunodeficiency virus. Sex was not considered in the study design. Donor sex and age information of each experiment was provided in Supplementary Table 5. Human PBMCs from the donors were isolated by centrifugation over lymphoprep[TM] according to the manufacturer's protocol and stored in liquid nitrogen. To enrich naïve human CD4^{+} T cells, cryopreserved PBMCs were thawed, washed, and negatively enriched using a MojoSort[TM] Human CD4^{+} Naïve T Cell Isolation Kit (BioLegend). Human CD4^{+} T cells were cultured in high glucose DMEM medium (Gibco), supplemented with 5% (v/v) heat-inactivated fetal bovine serum (FBS) and 2% (v/v) human AB serum (CellGro), 50 nM 2-mercaptoethanol (Gibco), 1 mM sodium pyruvate (Gibco), 1X MEM Non-Essential Amino Acids Solution (Gibco), 10 mM HEPES (Gibco), 1X L-Glutamine-Pen-Strep Solution (GeminiBio). The Institutional Review Board (IRB) of LJI approved the study.

Cell lines
HEK 293 T cells were purchased from ATCC and maintained according to the manufacturer's protocol.

Genotyping of eQTL
Genomic DNA was isolated from PBMC or gene edited human CD4^{+} T cells using the DNeasy Blood & Tissue Kit (QIAGEN). The *LACC1* promoter region was amplified with forward primer (5′-GAAACG

GCTTCCATTAGCAG-3') and reverse primer (5'-AGAGTTCCCTTCAG GATTTGC-3') with Phusion™ High-Fidelity DNA Polymerase (Thermo Scientific). Amplicons were purified with a NucleoSpin Gel and PCR Clean-up kit (MACHEREY-NAGEL) and sequenced by Sanger sequencing. rs12868462 (eQTL A) and rs3816311 (eQTL B) were sequenced with primer (5'-TTTAGTCCCGAGGTCGCTCC-3') from the forward direction. rs3215973 (eQTL C) and rs2275252 (eQTL D) were sequenced with primer (5'-CCACACTTAGCAATGACCAC-3') from the reverse direction.

Quantitative PCR

Total RNA was purified using the miRNeasy Micro Kit (QIAGEN). For human *LACC1* and mouse *Lacc1* mature mRNA quantification, reverse transcription of total RNA was performed with oligo(dT) primer, random hexamers and SuperScript™ III Reverse Transcriptase (Invitrogen). *LACC1* mature mRNA was quantified by real-time PCR using forward primer (5'-GGAATCAGCAGAGGCATTTC-3') and reverse primer (5'-CCTTGTGGCTTTACGGATGT-3'); *B2M* mature mRNA was quantified using forward primer (5'-CTGCCGTGTGAACCATGTGA CTTT-3') and reverse primer (5'-TGCGGCATCTTCAAACCTCCATG A-3'). *Lacc1* mature mRNA was quantified by real-time PCR using forward primer (5'-TGGGGTTGCTCACTCCGGCTG-3') and reverse primer (5'-GGAGACTGCTGATTCTTTGGGAAGA-3'); *B2m* mature mRNA was quantified using forward primer (5'-ACAGTTCCACCCGCCTCACATT-3') and reverse primer (5'-TAGAAAGACCAGTCCTTGCTGAAG-3'). All real-time PCR was performed with the Fast Start Universal SYBR Green Master Mix (Roche).

Quantification of *LACC1* pre-mRNA

LACC1 pre-mRNA was reverse transcribed from total RNA with random hexamers primers using SuperScript™ III Reverse Transcriptase (Invitrogen) and then amplified with forward primer (5'-GCAAATTGTCA CAGAGGTCG-3') and reverse primer (5'-AGAGTTCCCTTCAGG ATTTGC-3') using Phusion™ High-Fidelity DNA Polymerase (Thermo Scientific). Amplicons were sequenced with primer (5'-CCA-CACTTAGCAATGACCAC-3') from the reverse direction through Sanger sequencing. Transcripts from each allele were quantified by measuring the peak intensity at site D (rs2275252) using a SnapGene Viewer with software Version 6.2.1.

eQTL editing in human CD4⁺ T cells

Editing of the promoter eQTLs of *LACC1* was performed with CRISPR[25]. Briefly, naïve CD4⁺ T cells were enriched from human PBMCs and activated with Dynabeads Human T-Activator CD3/CD28 (Thermo Fisher Scientific) at a bead-to-cell ratio of 2:1 for 48 h. The beads were removed before transfection. RNP complexes were prepared by incubating dCas9 (IDT) with CRISPR RNA (crRNA) and trans activating crRNA (tracrRNA) duplex (IDT) specific for the target region for 20 min at room temperature. Then the activated CD4⁺ T cells were washed two times with PBS before resuspension in buffer T (IDT), and the editing template was added to the cell suspension along with RNP complex. Cells were transfected using the Neon Transfection System (Thermo Fisher Scientific) according to the manufacturer's protocol (settings: 1600 V, 10 ms, 3 pulses). After transfection, cells were activated with Dynabeads Human T-Activator CD3/CD28 at a bead-to-cell ratio of 1:1 for 24 h. The beads were removed and cells cultured in IL-2 containing medium for 3 days. eQTL-editing was verified by Sanger sequencing and *LACC1* gene expression was assessed by real-time PCR. Guide RNA sequences are provided in Supplementary Fig. 2.

BMDM differentiation

BMDMs were generated from total bone marrow cells isolated from mouse femora and tibiae and maintained in DMEM medium (Gibco) with 10% FBS, 1% penicillin/streptomycin (Gibco) and 50 ng/mL M-CSF (R&D) for 6 days. Cells were reseeded and stimulated with 5 ng/mL LPS

(Sigma) for 16 h. The culture supernatants were collected for TNF, IL-6 and IL-12p40 ELISA assays (BioLegend) according to the manufacturer's protocols.

T cell adoptive transfer colitis model

Mouse spleens were harvested, mashed in RPMI 1640 medium (Gibco) supplemented with 10% FBS and L-Glutamine-Pen-Strep Solution (GeminiBio), and filtered through 70 µm cell strainers (Fisherbrand). Red blood cells were lysed using Red Blood Cell Lysing Buffer Hybri-Max (Sigma-Aldrich). Cells were enriched with a Mojo-Sort Mouse CD4⁺ Naïve T Cell Isolation Kit (BioLegend) or EasySep Mouse CD4⁺ T Cell Isolation Kit (STEMCELL), and then stained with LIVE/DEAD Fixable Yellow Dead Cell Stain (Invitrogen), anti-mouse CD4 (RM4-5, BD Biosciences), CD45RB (16 A, BD Biosciences), and CD25 (PC61.5, eBioscience). Live CD4⁺CD45RB^high^CD25⁻ T cells and CD4⁺CD45RB^low^CD25⁺ Treg cells were sorted on a BD FACSAria cell sorter (BD Biosciences). For T cell transfer experiments, 2.5×10^5 CD4⁺CD45RB^high^CD25⁻ T cells were injected into *Rag1*⁻/⁻ mice retroorbitally. For co-transfer experiments, 2×10^5 CD4⁺CD45RB^high^CD25⁻ T cells and 1×10^5 Treg cells were injected into *Rag1*⁻/⁻ mice retroorbitally. Mouse health, including hunched back, other behaviors, and diarrhea were monitored daily. Body weights of *Rag1*⁻/⁻ mice were measured weekly and the mice were euthanized when they lost 20% of their weight or showed deteriorated health. Colons of the mice was fixed with Zinc Formalin for H&E staining and histology analysis.

DSS colitis model

DSS MW ca 40,000 (Alfa Aesar) 2.5% (w/v) was added to the drinking water of mice with free access. Mouse health and symptoms of diarrhea and bleeding were monitored daily. Body weights of the mice were measured daily and the mice were euthanized when they lost 20% of their weight or showed a moribund condition. Colons of the mice were fixed with Zinc Formalin for H&E staining and histology analysis.

Histology scoring of colitis

Histology scoring tissues from the T cell transfer colitis and DSS colitis models were established based on previous studies[43,44]. Briefly, T cell transfer colitis was scored based on the severity of inflammatory infiltration, goblet cell loss, crypt density, crypt hyperplasia, muscle thickening, and submucosal inflammation. DSS colitis was scored based on severity of inflammation, area of infiltration, crypt damage and edema. Details are included in Supplementary Table 4.

Mouse Treg cell in vitro differentiation

Naïve CD4⁺ T cells were enriched from mouse spleen with a MojoSort Mouse CD4⁺ Naïve T Cell Isolation Kit (BioLegend). 1×10^5 cells were seeded into each well of a 96-well plate pre-coated with 1 µg/mL purified anti-mouse CD3ε antibody (Clone 145-2C11, BioLegend) in 200 µl RPMI medium (Gibco) containing 10% FBS, 1% penicillin/streptomycin (Gibco), 1 µg/mL purified anti-mouse CD28 antibody (Clone 37.51, BioLegend) and 1 ng/mL human recombinant TGFβ (R&D Systems). Three days later, cells were reseeded into each well of a 96-well plate pre-coated with 1 µg/mL purified anti-mouse CD3ε antibody in 200 µl RPMI medium containing 10% FBS, 1% penicillin/streptomycin, 1 ng/mL human TGFβ and 25 ng/mL mouse recombinant IL-2 (R&D Systems) and cultured for another 4 days before analysis.

Plasmids and molecular cloning

pLKO.1-GFP vector was adapted from the pLKO.1 puro vector (Plasmid #8453, Addgene) by replacing the Puromycin resistant gene with a gene encoding green fluorescent protein. shRNA sequences of *LACC1* (5'TGCTGTTGACAGTGAGCGCAGACTTTGAATGCTGTCCAATTAG TGAAGCCACAGATGTAATTGGACAGCATTCAAAGTCTTTGCCTACTG CCTCGGA-3')

or *CD45*

(5'TGCTGTTGACAGTGAGCGAGCAGATGATCTTCCAAAGAAATA
GTGAAGCCACAGATGTATTTCTTTGGAAGATCATCTGCCTGCCTACT
GCCTCGGA-3')

were inserted into the AgeI and EcoRI sites of pLKO.1-GFP. Lentiviral packaging plasmids psPAX2 (Plasmid #12260) and pMD2.G (Plasmid #12259) were obtained from Addgene.

Lentiviral packaging

1×10^6 HEK 293 T cells (ATCC) were plated on a 60 mm cell culture dish in high glucose DMEM medium (Gibco), supplemented with 10% heat-inactivated fetal bovine serum (FBS), 10 mM HEPES (Gibco), 1X L-Glutamine-Pen-Strep Solution (GeminiBio). After 24 h, when confluency reached 90%, cells were transfected with the lentiviral packaging plasmid cocktail, which was made by mixing 20 µl TransIT-LT1 Transfection Reagent (Mirus Bio) and 10 ug plasmids (2.4 ug pMD2.G, 4.5 ug psPAX2, 3.1 ug pLKO.1-GFP) in 500 µl Opti-MEM™ Reduced Serum Medium (Gibco) and incubated at room temperature for 30 min. 24 h after transfection, the culture medium was replaced by fresh medium. 48 h and 72 h after transfection, the culture supernatant containing lentivirus was harvested and filtered through a 0.45 um surfactant-free cellulose acetate membrane Nalgene filter (Thermo Scientific). The virus was stored at -80 C°.

Lentiviral transduction of human CD4⁺ T cells

Naïve CD4⁺ T cells were enriched from human PBMCs. 5×10^5 cells were seeded into each well of a 24-well plate pre-coated with 5 µg/mL purified anti-human CD3 antibody (Clone UCHT1, BioLegend) in 500 µl human T cell culture medium containing 2.5 µg/mL purified anti-human CD28 antibody (Clone CD28.2, BioLegend). 24 h after activation, the supernatant was replaced with medium containing shRNA-expressing lentivirus. The culture plate was centrifuged at 800 *g* for 2 h at room temperature and then incubated in the 37 °C incubator for 2 h. After transduction, the virus medium was replaced by T cell culture medium containing 2.5 µg/mL purified anti-human CD28 antibody and the cells were activated for another 48 h. Finally, the cells were expanded in T cell culture medium containing 10 ng/mL human recombinant IL-2 (BioLegend). Transduction efficiency was assessed by measuring GFP expressing cells by flow cytometry. Knockdown of *LACC1* was assessed by real-time PCR and Western blotting.

Western blotting

T cells were harvested and washed once in PBS, and lysed on ice for 15 min in RIPA Lysis and Extraction Buffer (Thermo Scientific) supplemented with Halt Protease and Phosphatase Inhibitor Cocktail (Thermo Scientific). The cell lysate was centrifuged at 14,000 *g* for 15 min at 4 C°. Protein concentration of the supernatant was measured using the BCA Protein Assay (Thermo Scientific). Proteins were denatured by boiling for 10 min in SDS sample loading buffer and then loaded on 12% SDS-PAGE gel for electrophoresis, followed by transfer to a polyvinylidene difluoride transfer membrane (Santa Cruz). The membrane was blocked with 5% non-fat milk in Tris Buffered Saline with 0.01%Tween 20 (TBST, ChemCruz) buffer and incubated with the primary antibody overnight at 4 C°. Mouse anti-LACC1 antibody (E-12) was obtained from Santa Cruz, and rabbit anti-HSP90 antibody was obtained from Cell Signaling. The membrane was washed with Tris-buffered saline with 0.1% Tween® 20 detergent (TBST) 3 times and incubated in horse radish peroxidase (HRP)-conjugated secondary antibody (Cell Signaling). The membrane containing heat shock protein (HSP)90 was processed with the Western Blotting Luminol Reagent (Santa Cruz Biotechnology). The membrane containing LACC1 was processed with a WesternBright ECL kit (Advansta). The membranes were exposed to Blue X-Ray films (Phenix) and the films were scanned for analysis.

Oxygen consumption rate and extracellular acidification rate

Seahorse XF Cell Mito Stress Test Kit, Seahorse XF Glycolysis Stress Test Kit, XF Sensor Cartridges & Cell Culture Microplates, and a Seahorse XF Analyzer were obtained from Agilent. The 96-well cell culture microplates were pre-coated with Poly-D-Lysine (Gibco). T cells were washed and then plated on the microplates at 2×10^5 cells/well in 180 µl of Seahorse XF DMEM assay medium pH 7.4 (Agilent) which was supplemented with 1 mM pyruvate (Agilent), 2 mM glutamine (Agilent). 25 mM glucose was supplemented in the medium in the Cell Mito Stress Test. After incubation at 37°C in a non-CO₂ incubator for 45 minutes, the microplates were loaded to the calibrated Seahorse XF Analyzer for measurement of the oxygen consumption rate and extracellular acidification rate. For Cell Mito Stress Test, 15 uM oligomycin, 10 uM carbonyl cyanide-p-trifluoromethoxyphenylhydrazone (FCCP) and 5 uM Rot/AA were loaded into the cartridge port. For the Glycolysis Stress Test, 100 mM glucose, 10 uM oligomycin and 500 mM 2-deoxy glucose (2-DG) were loaded into the cartridge port. For each sample, 3-5 technical replicates were measured and average values were used for statistics. Data analysis was performed according to the manufacturer's instruction.

Metabolite extraction and LC-MS analysis

Cultured *LACC1* EV and KD Th0 cells were incubated in DMEM (glucose-free formulation) containing 10 mM [U-¹³C] glucose (Cambridge Isotope Laboratories), 2 mM glutamine, 5% dialyzed FBS (Thermo Fisher) at 37 °C for 16 h. 1×10^6 cells were harvested and washed in 150 mM of ice-cold ammonium acetate, pH 7.3, and metabolites were extracted in 80% methanol on dry ice before evaporation under vacuum. For the negative ion mode, dried metabolites were resuspended in 50 µl of 50% acrylonitrile (ACN), and 5 µl was injected for chromatographic separation using the Ion Chromatography System 5000 (Thermo Fisher) coupled to a Q Exactive run in negative polarity mode (Thermo Fisher). Source settings were S-lens, 50; Sheath Gas, 18; Aux Gas, 4; spray heater, 320 °C; and spray voltage, −3.2 kV or ⁺3.2 kV. Metabolites were identified based on accurate mass (± 3 ppm) and retention times of pure standards. For the positive ion mode, dried metabolites were resuspended in 40 µl 50% ACN:water and 5 µl was loaded onto a Luna 3um NH2 100 A (150 × 2.0 mm) column (Phenomenex). The chromatographic separation was performed on a Vanquish Flex (Thermo Scientific) with mobile phases A (5 mM NH4AcO pH 9.9) and B (ACN) and a flow rate of 200 µl/min. A linear gradient from 15% A to 95% A over 18 min was followed by 7 min isocratic flow at 95% A and re-equilibration to 15% A. Metabolites were detected with a Thermo Scientific Q Exactive mass spectrometer run with polarity switching in full scan mode with an m/z range of 70–975 and 70.000 resolution. Maven (v 8.1.27.11) was utilized to quantify the targeted metabolites by AreaTop using accurate mass measurements (<5 ppm), and the expected retention time previously verified with standards. Relative amounts of metabolites were calculated by summing up the values for all isotopologues of a given metabolite. C13 natural abundance corrections were made using AccuCor.

Cell proliferation assay

Naïve CD4⁺ T cells were enriched from human PBMCs and stained with CellTrace Violet Cell Proliferation Kit (Invitrogen) according to manufacturer's protocol. Then cells were divided into different wells for different transduction and culture conditions as described above. 10 days after culturing in the Th0 condition, CellTrace Violet (CTV) was measured through flow cytometry and quantified by mean fluorescence intensity (MFI).

T helper cell in vitro differentiation

Naïve CD4⁺ T cells were enriched from human PBMCs. 1×10^5 cells were seeded into each well of a 96-well plate pre-coated with 5 µg/mL purified anti-human CD3 antibody (Clone UCHT1, BioLegend) in 200 µl

human T cell culture medium containing 2.5 µg/mL purified anti-human CD28 antibody (Clone CD28.2, BioLegend) and cytokine polarization cocktails. 24 h after activation, the supernatant was replaced with medium containing shRNA-expressing lentivirus for transduction. After transduction, the virus medium was replaced by T cell culture medium containing anti-human CD28 antibody and cytokine polarization cocktails for another 48 h. The cells were expanding in fresh T cell polarization medium for 4 days, and were split as needed every 2 days. Th0 cell polarization medium contained 5 ng/mL IL-2 (BioLegend). Th1 cell polarization medium contained 5 ng/mL human IL-12 (R&D Systems), 5 ng/mL IL-2 (BioLegend), 5 µg/mL anti-human IL-4 (Clone MP4-25D2, eBioscience). Treg cell polarization medium contained 5 ng/mL IL-2 (BioLegend), and doses of human TGFβ from 0 to 5 ng/mL (R&D Systems). Th17 cell polarization medium contained 50 ng/mL human IL-1β (R&D Systems), 50 ng/mL IL-23 (R&D Systems), 5 ng/mL human TGFβ (R&D Systems), 5 µg/mL anti-human IL-4 (Clone MP4-25D2, eBioscience), 10 µg/mL anti-human IFNγ (Clone NIB42, eBioscience).

Human induced Treg in vitro suppression assay
Human Treg were differentiated and transduced using the methods above in 5 ng/mL human TGFβ for 4 days. T effector cells were naïve CD4+ T cells enriched from human PBMCs, stained with CellTrace Violet (Thermo Fisher) and then co-cultured with Treg cells. 5×10^4 naïve CD4+ T cells were co-cultured with induced Treg cells at different ratios in each well of a 96-well plate in 200 µl human T cell culture medium containing 2 µg/mL purified anti-human CD3 antibody and 5 ng/mL human IL-2. 5 day later, T effector cell proliferation were determined by flow cytometry measurement of CellTrace Violet.

RNA sequencing
RNA sequencing libraries were prepared using the Smart-seq2 protocol[45]. Total RNA was purified using the miRNeasy Micro Kit (QIAGEN). cDNA was reverse transcribed from total RNA with oligo(dT) primer, random hexamers with SuperScript™ II Reverse Transcriptase (Invitrogen) and then amplified with IS PCR primers and Kapa HiFi Hotstart Ready Mix (Roche). Then the cDNA library was fragmented and tagged with sequencing adapters using Nextera XT DNA Library Preparation Kit (Illumina), and finally ~500 bp amplicons were obtained. Library quality was assessed using the High Sensitivity RNA ScreenTape Kit (Agilent Life Sciences). DNA was quantified using Quant-iT PicoGreen dsDNA Assay Kits (Invitrogen) and purified using AMPure XP beads (Beckman Colter). Libraries were subjected to 2 × 50-bp paired-end sequencing on an Illumina NovaSeq6000 (Illumina), generating at least 8 million uniquely mapped reads for each sample.

RNA-seq analysis
Reads were mapped to the hg19 reference genome using STAR with the LJI in-house pipeline (https://github.com/ndu-UCSD/LJI_RNA_SEQ_PIPELINE_V2). After quality control, 18 of 20 samples remained with at least 80% of mapping reads were selected. Differential gene expression between empty vector (EV) and *LACC1* Knock-down (KD) for each T cell type was performed using DESeq2 (v1.38.3) in an R environment (v4.2.2). To perform donor paired analysis between samples, 5 pairs of samples were used for the Th0 cell analysis, 4 pairs of samples were used for the Treg cells. Significant differential expression was defined as $\log_2$ Fold-Change higher than 1.0 and a Benjamini-Hochberg-adjusted *p*-value lower than 0.05. The differentially expressed gene analysis results were provided in the Supplementary Data 1 and 2. Gene set enrichment analysis (GSEA) was performed using fgsea package (v.1.24.0) for either the Hallmark or C7 (Immunologic signatures) gene sets from the Human MSigDB (gsea-msigdb.org) considering a false-discovery-rate (FDR) lower than 0.05.

Flow cytometry
T cells were prepared in staining buffer (PBS with 2% FBS and 2 mM EDTA), human IgG (Sigma Aldrich), and surface proteins were stained with antibodies as indicated below for 15 min at 4 °C. Cell viability was determined using LIVE/DEAD Fixable Yellow Dead Cell Stain (Invitrogen). For cytokine staining, cells were treated with PMA (Sigma Aldrich), Ionomycin (Sigma Aldrich) and BFA (Sigma Aldrich) for 4 h. For intracellular cytokine or transcription factor staining, cells were fixed with Cytofix Fixation Buffer (BD Biosciences) and then stained with Foxp3 / Transcription Factor Staining Buffer Set (eBioscience) at 4 °C. The following antibodies from BD Biosciences, BioLegend or eBioscience were used: anti-human CD4 (OKT4), CD4 (RPA-T4), CD8α (RPA-T8), CD25 (2A3), CD3 (UCHT1), CD45RA (HI100), CD45RO (UCHL1), CD45 (HI30), FoxP3 (PCH101), IL-17A (BL168), IFNγ (4S.B3), TNF (MAb11), IL-2 (MQ1-17H12), IL-10 (JES3-9D7); anti-mouse CD4 (RM4-5), TCRβ (H57-597), CD8α (53-6.7), CD44 (IM7), CD62L (MEL-14), FoxP3 (FJK-16s), IL-17A (TC11-18H10), IFNγ (XMG1.2), TNF (MP6-XT22), IL-10 (JES5-16E3), IL-2 (JES6-5H4), IL-4 (11B11). The antibody dilution and catalog information were provided in Supplementary Table 6. All samples were acquired on a BD LSR II flow cytometer or sorted on a BD FACSAria cell sorter (both BD Biosciences) and analyzed using FlowJo 10.4.1.

Quantification and statistical analysis
The number of subjects, samples or mice/group, replication in independent experiments, and statistical tests can be found in the figure legends. Details on quality control, sample elimination and displayed data are stated the Method details and figure legends. Sample sizes were chosen based on published studies to ensure sufficient numbers of mice or human donors in each group enabling reliable statistical testing and accounting for variability. RNA-seq samples that didn't pass quality control were not included in the analyzes. Animal experiments were reproduced in at least two independent experiments. Animals of same sex and age were randomly assigned to experimental groups. Statistical analyzes were performed with Graph Pad Prism 9.

Reporting summary
Further information on research design is available in the Nature Portfolio Reporting Summary linked to this article.

Data availability
All data supporting the findings of this study are provided in the Supplementary Information and Source Data file. The RNA-seq datasets have been deposited in the NCBI GEO database under primary accession number GSE272811. For the transcriptomic analysis, reads were mapped to to hg19 (v3.0.0) for human data. Source data are provided with this paper.

Code availability
Scripts used for this paper and explanations thereof are available at the GitHub repository (https://github.com/gabrielascui/lacc1).

References
1. Franke, A. et al. Genome-wide meta-analysis increases to 71 the number of confirmed Crohn's disease susceptibility loci. *Nat. Genet* **42**, 1118–1125 (2010).
2. Jostins, L. et al. Host-microbe interactions have shaped the genetic architecture of inflammatory bowel disease. *Nature* **491**, 119–124 (2012).
3. Liu, J. Z. et al. Association analyses identify 38 susceptibility loci for inflammatory bowel disease and highlight shared genetic risk across populations. *Nat. Genet* **47**, 979–986 (2015).

4. de Lange, K. M. et al. Genome-wide association study implicates immune activation of multiple integrin genes in inflammatory bowel disease. *Nat. Genet* **49**, 256–261 (2017).

5. Cader, M. Z. et al. C13orf31 (FAMIN) is a central regulator of immunometabolic function. *Nat. Immunol.* **17**, 1046–1056 (2016).

6. Umeno, J. et al. Meta-analysis of published studies identified eight additional common susceptibility loci for Crohn's disease and ulcerative colitis. *Inflamm. Bowel Dis.* **17**, 2407–2415 (2011).

7. Barrett, J. C. et al. Genome-wide association defines more than 30 distinct susceptibility loci for Crohn's disease. *Nat. Genet* **40**, 955–962 (2008).

8. Assadi, G. et al. LACC1 polymorphisms in inflammatory bowel disease and juvenile idiopathic arthritis. *Genes Immun.* **17**, 261–264 (2016).

9. Omarjee, O. et al. LACC1 deficiency links juvenile arthritis with autophagy and metabolism in macrophages. *J. Exp. Med.* **218**, e20201006 (2021).

10. Patel, N. et al. Study of Mendelian forms of Crohn's disease in Saudi Arabia reveals novel risk loci and alleles. *Gut* **63**, 1831–1832 (2014).

11. Wakil, S. M. et al. Association of a mutation in LACC1 with a monogenic form of systemic juvenile idiopathic arthritis. *Arthritis Rheumatol.* **67**, 288–295 (2015).

12. Rabionet, R. et al. Biallelic loss-of-function LACC1/FAMIN mutations presenting as rheumatoid factor-negative polyarticular juvenile idiopathic arthritis. *Sci. Rep.* **9**, 4579 (2019).

13. Karacan, I. et al. LACC1 gene defects in familial form of juvenile arthritis. *J. Rheumatol.* **45**, 726–728 (2018).

14. Kallinich, T. et al. Juvenile arthritis caused by a novel FAMIN (LACC1) mutation in two children with systemic and extended oligoarticular course. *Pediatr. Rheumatol. Online J.* **14**, 63 (2016).

15. Liu, H. et al. Discovery of six new susceptibility loci and analysis of pleiotropic effects in leprosy. *Nat. Genet* **47**, 267–271 (2015).

16. Takeuchi, M. et al. Dense genotyping of immune-related loci implicates host responses to microbial exposure in Behçet's disease susceptibility. *Nat. Genet* **49**, 438–443 (2017).

17. Schmiedel, B. J. et al. Impact of genetic polymorphisms on human immune cell gene expression. *Cell* **175**, 1701–1715 e16 (2018).

18. Cader, M. Z. et al. FAMIN is a multifunctional purine enzyme enabling the purine nucleotide cycle. *Cell* **180**, 278–295.e23 (2020).

19. Wei, Z. et al. LACC1 bridges NOS2 and polyamine metabolism in inflammatory macrophages. *Nature* **609**, 348–353 (2022).

20. Lahiri, A. et al. Human LACC1 increases innate receptor-induced responses and a LACC1 disease-risk variant modulates these outcomes. *Nat. Commun.* **8**, 15614 (2017).

21. Huang, C. et al. LACC1 required for NOD2-induced, ER stress-mediated innate immune outcomes in human macrophages and LACC1 risk variants modulate these outcomes. *Cell Rep.* **29**, 4525–4539 (2019).

22. Kang, J. W. et al. Myeloid cell expression of LACC1 is required for bacterial clearance and control of intestinal inflammation. *Gastroenterology* **159**, 1051–1067 (2020).

23. Hugot, J. P. et al. Association of NOD2 leucine-rich repeat variants with susceptibility to Crohn's disease. *Nature* **411**, 599–603 (2001).

24. Xu, Z. Y. & Wang, J. C. LACC1 regulates changes in the intestinal flora in a mouse model of inflammatory bowel disease. *BMC Gastroenterol.* **23**, 358 (2023).

25. Chandra, V. et al. Promoter-interacting expression quantitative trait loci are enriched for functional genetic variants. *Nat. Genet* **53**, 110–119 (2021).

26. Stewart, A. J., Hannenhalli, S. & Plotkin, J. B. Why transcription factor binding sites are ten nucleotides long. *Genetics* **192**, 973–985 (2012).

27. Skon-Hegg, C. et al. LACC1 regulates TNF and IL-17 in mouse models of arthritis and inflammation. *J. Immunol.* **202**, 183–193 (2019).

28. Hall, L. J. et al. Induction and activation of adaptive immune populations during acute and chronic phases of a murine model of experimental colitis. *Dig. Dis. Sci.* **56**, 79–89 (2011).

29. Chassaing, B. et al. Dextran sulfate sodium (DSS)-induced colitis in mice. *Curr. Protoc. Immunol.* **104**, 15 25 1–15 25 14 (2014).

30. MacIver, N. J., Michalek, R. D. & Rathmell, J. C. Metabolic regulation of T lymphocytes. *Annu Rev. Immunol.* **31**, 259–283 (2013).

31. Kerdiles, Y. M. et al. Foxo transcription factors control regulatory T cell development and function. *Immunity* **33**, 890–904 (2010).

32. Ouyang, W. et al. Foxo proteins cooperatively control the differentiation of Foxp3+ regulatory T cells. *Nat. Immunol.* **11**, 618–627 (2010).

33. Plitas, G. et al. Regulatory T cells exhibit distinct features in human breast cancer. *Immunity* **45**, 1122–1134 (2016).

34. Michalek, R. D. et al. Cutting edge: distinct glycolytic and lipid oxidative metabolic programs are essential for effector and regulatory CD4+ T cell subsets. *J. Immunol.* **186**, 3299–3303 (2011).

35. Huber, S. et al. P38 MAP kinase signaling is required for the conversion of CD4+CD25- T cells into iTreg. *PLoS One* **3**, e3302 (2008).

36. Huang, H. et al. Fine-mapping inflammatory bowel disease loci to single-variant resolution. *Nature* **547**, 173–178 (2017).

37. Perlman, R. L. Mouse models of human disease: an evolutionary perspective. *Evol. Med Public Health* **2016**, 170–176 (2016).

38. Zheng-Bradley, X. et al. Large scale comparison of global gene expression patterns in human and mouse. *Genome Biol.* **11**, R124 (2010).

39. Berg, D. J. et al. Enterocolitis and colon cancer in interleukin-10-deficient mice are associated with aberrant cytokine production and CD4(+) TH1-like responses. *J. Clin. Invest* **98**, 1010–1020 (1996).

40. Wu, R. et al. De novo synthesis and salvage pathway coordinately regulate polyamine homeostasis and determine T cell proliferation and function. *Sci. Adv.*, **6**, eabc4275 (2020).

41. Puleston, D. J. et al. Polyamine metabolism is a central determinant of helper T cell lineage fidelity. *Cell* **184**, 4186–4202 e20 (2021).

42. Mayne, C. G. & Williams, C. B. Induced and natural regulatory T cells in the development of inflammatory bowel disease. *Inflamm. Bowel Dis.* **19**, 1772–1788 (2013).

43. Eschweiler, S. et al. Intermittent PI3Kdelta inhibition sustains antitumour immunity and curbs irAEs. *Nature* **605**, 741–746 (2022).

44. Dicker, M. et al. CD4(+)-mediated colitis in mice is independent of the GPR183 and GPR18 pathways. *Front Immunol.* **13**, 1034648 (2022).

45. Picelli, S. et al. Full-length RNA-seq from single cells using Smart-seq2. *Nat. Protoc.* **9**, 171–181 (2014).

Acknowledgements

Author contributions

Y.L.: study design, experimental work, data interpretation, paper writing; G.A.: bioinformatic evaluation, data interpretation, paper review; M.D.: experimental work, paper review; T.R.: data interpretation, paper review;

V.C.: study design, data interpretation, paper review; B.S.: study design, paper review; T.C.: experimental work, paper review; P.V., M.K.: study design, data interpretation, paper writing, supervised and led the work.

Competing interests

The authors declare no competing interests.

Additional information